JACS
JOURNAL OF THE AMERICAN CHEMICAL SOCIETY

COMMUNICATION

pubs.acs.org/JACS

Hydrothermal Synthesis of Zeolites with Three-Dimensionally Ordered Mesoporous-Imprinted Structure

Huiyong Chen,[†,§] James Wydra,[†] Xueyi Zhang,[†] Pyung-Soo Lee,[†] Zhuopeng Wang,[‡] Wei Fan,[*,‡] and Michael Tsapatsis[*,†]

[†]Department of Chemical Engineering and Materials Science, University of Minnesota, Minneapolis, Minnesota 55455, United States
[‡]Department of Chemical Engineering, University of Massachusetts, Amherst, Massachusetts 01003, United States
[§]School of Chemistry and Chemical Engineering, South China University of Technology, Guangzhou, China 510640

Supporting Information

ABSTRACT: Zeolites are microporous materials with pores and channels of molecular dimensions that find numerous applications in catalysis, separations, ion exchange, etc. However, whereas uniformity of micropore size is a most desirable and enabling characteristic for many of their uses, in certain cases, for example in reactions involving bulky molecules, it is a limitation. For this reason, synthesis of hierarchical zeolites with micro- and mesoporosity is of considerable interest as a way to control molecular traffic for improved catalytic and separation performance. Herein, we report a general synthesis route for the confined synthesis of zeolites within three-dimensionally ordered mesoporous carbon templates by conventional hydrothermal synthesis. Various zeolites, including BEA, LTA, FAU, and LTL, with three-dimensionally ordered mesoporous-imprinted structure have been synthesized by this approach. It is expected that these hierarchical zeolite materials will provide building blocks for thin-film and other syntheses and may provide a basis for quantitatively studying the mass-transfer limitation on the catalytic performance of zeolite catalysts.

Due to their ordered micropore structures and acid strength, zeolites are extensively used as heterogeneous acid catalysts in refineries and petrochemical processes.[1] However, their micropore structures and high intrinsic activities frequently make these materials subject to diffusion limitations that, for example, restrict reactant accessibility to the active sites on the interior surfaces of zeolites and inhibit the full utilization of zeolite catalysts.[2] Nanofabrication of hierarchical zeolite catalysts with mesoporosity is a proven strategy for integrating shape selectivity (provided by the intrinsic micropore structures) and efficient mass transfer (facilitated by the mesopore structures).[3] Considerable efforts have been devoted to the synthesis of zeolite catalysts with mesoporosity, including dealumination,[4] desilication,[5] recrystallization of zeolites,[6] assembly of zeolite nanocrystals,[7] soft template methods,[8] and confined synthesis in hard templates.[9] Among them, the synthesis of hierarchical zeolites by confined synthesis in hard templates holds exciting implications for creating ordered mesoporous structures and controlling mesopore sizes with precisions unattainable by the other methods. In principle, the desired mesopore structure can be achieved by manipulating the structure of the hard template. These advantages provide unique opportunities to design the hierarchical pore structure and quantitatively investigate the effects of mesopore structure on the catalytic performance of zeolite catalysts.

Recently, we have demonstrated that hierarchical zeolites can be realized through confined growth within three-dimensionally ordered mesoporous (3DOm) carbon by a steam-assisted crystallization (SAC) method.[10] Three-dimensionally ordered mesoporous-imprinted (3DOm-i) single-crystal ZSM-5 and size-tunable zeolite nanocrystal silicalite-1 have been synthesized by this method for applications in catalysis[11] and the manufacture of thin zeolite membranes for separations.[12] In the SAC method, incipient-wetness techniques were used to impregnate the 3DOm carbon with a zeolite synthesis solution. Because the pore volume of the 3DOm carbon was approximately the same as the volume of the synthesis solutions that were added, nucleation and crystal growth were mostly confined in the interior space of 3DOm carbon. 3DOm-i zeolite crystals are composed of uniform zeolitic spherical elements with their size limited by the spherical mesopore size of the 3DOm carbon used in their synthesis. Many similarly oriented and interconnected spherical elements form single zeolite crystals, as shown in Figure 1.

The SAC method was first developed for the synthesis of MFI.[13] Since then, a few zeolites, including zeolite MOR, FER, BEA, EMT, and FAU, have been successfully synthesized by this method.[14] Compared to conventional hydrothermal (HT) synthesis methods, the available methods for making zeolites from SAC method are rather limited and often require preparation of dense gels which cannot penetrate 3DOm carbon. Therefore, to extend the list of available 3DOm-i zeolites, we developed a straightforward approach to synthesize zeolites inside 3DOm carbon under conventional HT conditions. The challenge for zeolite growth inside the 3DOm carbon by HT methods is to hinder crystal formation outside while allowing zeolite growth inside the 3DOm carbon. It turned out that this challenge can be overcome by seeded growth. First, zeolite seeds were grown inside the 3DOm carbon under optimized HT conditions. Crystal growth was subsequently carried out by adding the seeded 3DOm carbon into a freshly prepared synthesis solution. The process was repeated several times until the formation of a considerable amount of zeolite inside the 3DOm carbon was achieved. By

Received: May 22, 2011
Published: July 18, 2011

dx.doi.org/10.1021/ja2046815 | J. Am. Chem. Soc. 2011, 133, 12390–12393

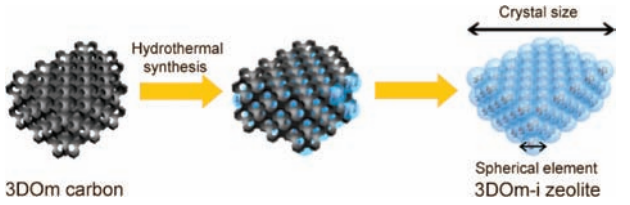

Figure 1. Schematic of formation of 3DOm-i zeolite confined in the pore space of 3DOm carbon.

systematic variation of the synthesis parameters, 3DOm-i zeolites with BEA, LTA, FAU, and LTL topologies have been synthesized by this approach.

As a hard template in the synthesis process, 3DOm carbon with a pore size from around 10 to 40 nm was obtained by replication from colloidal crystals composed of size-tunable silica nanoparticles according to previous reports.[10,15] For the confined growth of zeolites in the 3DOm carbon, it is essential to allow the nutrients needed for zeolite formation to access the mesopores. For this reason, clear synthesis solutions were used in the syntheses.

For the case of 3DOm-i zeolite beta (3DOm-i BEA), 3DOm carbon was immersed into a clear solution with a composition of $0.35Na_2O{:}4.5(TEA)_2O{:}0.25Al_2O_3{:}25SiO_2{:}330H_2O$, followed by HT synthesis at 100 °C for 4 days.[16] After the first synthesis cycle, the carbon template was washed with distilled water and re-immersed in a freshly prepared synthesis solution for the next synthesis cycle at 100 °C for 4 days. X-ray diffraction (XRD) at wide angles shows weak diffraction peaks from the sample after the first synthesis cycle (Figure S1). The peaks become more intense after the second cycle and continuously increase in intensity with additional synthesis cycles. The XRD patterns in Figure 2a confirm that 3DOm-i BEA can be prepared after four HT cycles in 3DOm carbons with mesopores ranging from 10 to 40 nm. It is found that the diffraction peak at 22.7°, associated with the (302) reflection of zeolite beta, is slightly broadened with decreasing pore size of the 3DOm carbon. The broad peak around 7.5° is composed of the (100) and (101) reflections of zeolite beta, indicating a highly faulted intergrown structure of A and B polymorphs. The crystal structure is well retained after removal of the 3DOm carbon template at 550 °C, although a decrease in the intensity of the peak at 22.7° is observed (Figure S2). The phenomenon was also observed in the synthesis of zeolite beta without using the carbon template and is attributed to the removal of the organic structure-directing agent (SDA) (Figure S3).[17] XRD at a low angle after carbon removal (Figure 2b) reveals that the 3DOm-i BEA samples retain a high degree of mesostructural ordering imprinted from the 3DOm carbon. The low-angle XRD patterns of the 3DOm-i BEA samples formed after each HT cycle also reveal the gradual development of an ordered mesostructure during the synthesis (Figure S1). After the diffraction peaks at low angle were indexed according to a face-centered-cubic structure, the center-to-center distances between the spherical zeolite elements were calculated (from Bragg's law using the lowest angle peak as (111)) to be 12, 20, and 37 nm, in agreement with the corresponding pore size of the 3DOm carbon template used and the expected nominal spherical element size of 3DOm-i BEA confirmed by transmission electron microscopy (TEM, Figure 2d–f).

The presence of mesoporosity in the 3DOm-i BEA was confirmed by the nitrogen adsorption–desorption isotherms

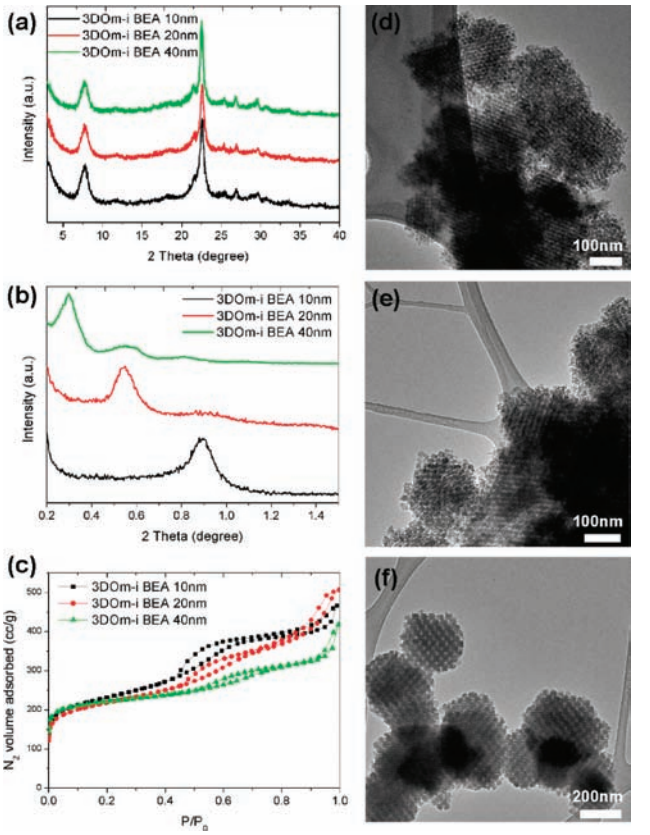

Figure 2. Characterization of the 3DOm-i BEA formed within the 3DOm carbon templates. (a) Wide-angle XRD of the 3DOm-i BEA samples before the removal of carbon template. (b) Low-angle XRD and (c) nitrogen adsorption–desorption isotherms after the carbon was removed by calcination. (d–f) TEM images of the 3DOm-i BEA formed within 10, 20, and 40 nm 3DOm carbon, respectively.

as shown in Figure 2c. It is found that the hysteresis in the nitrogen adsorption–desorption isotherms is shifted to higher P/P_0 with increasing mesopore size of the 3DOm carbon, reflecting the correspondingly larger mesopore sizes in the respective 3DOm-i BEA. BJH pore size analysis (Figure S4) further underscores the presence of marked mesoporosity in the 3DOm-i BEA. Textural analysis (Table S1) reveals that the micropore volume of 3DOm-i BEA zeolites is similar to that of conventional zeolites, indicating that the micropore structure of 3DOm-i zeolite is retained during the confined growth.

To further explore the feasibility of this synthesis approach, attempts have been made to synthesize 3DOm-i zeolite LTA, FAU, and LTL in the 3DOm carbon template by changing the initial synthesis solutions and synthesis parameters.[18] (Detailed synthesis procedures are described in the Supporting Information.) The mesostructure is clearly observed in the representative TEM images of 3DOm-i LTA FAU and LTL (Figure 3). XRD patterns at wide and low angle (Figure S5) reveal the signature reflections of LTA and of an ordered mesostructure, respectively. Selected-area electron diffraction (SAED, Figure 3a inset) of the 3DOm-i LTA sample clearly shows a single-crystal diffraction pattern. As discussed before, the formation of these single zeolite crystals probably starts from the nucleation in one or more adjacent cages of the 3DOm carbon and is followed by growth propagating from cage to cage through the connecting windows to nearly complete filling of the neighboring cages.[10] Similar results were observed for the case

dx.doi.org/10.1021/ja2046815 |J. Am. Chem. Soc. 2011, 133, 12390–12393

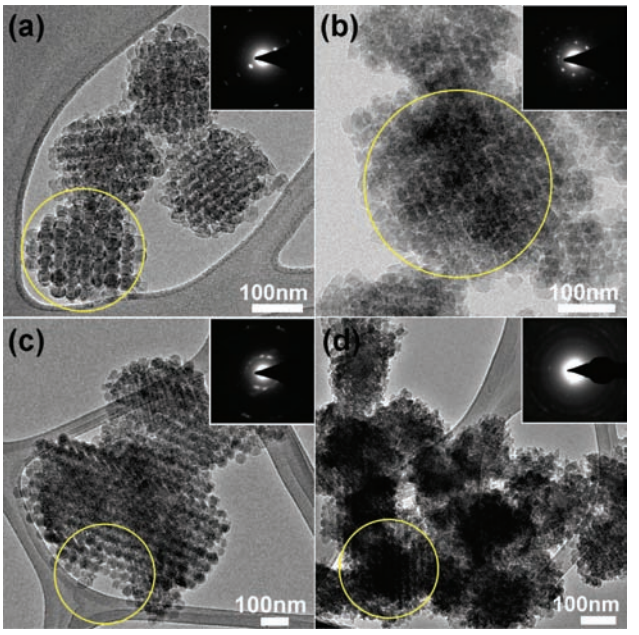

Figure 3. 3DOm-i zeolite crystals. TEM images of 3DOm-i LTA (a), FAU (b), BEA (c), and LTL (d) grown within a 40 nm 3DOm carbon template. Insets: electron diffraction patterns from the circled areas in the corresponding TEM images.

of 3DOm-i FAU (XRD pattern and HRTEM image of 3DOm-i FAU are shown in Figures S6 and S7, respectively) and 3DOm-i BEA, as shown in the insets of Figure 3b,c.

The case for LTL zeolite however, was different. A homogeneous potassium aluminosilicate solution without organic SDA was used to prepare zeolite LTL within the 3DOm carbon. The TEM image in Figure 3d clearly reveals that zeolite LTL crystals are formed within the 40 nm 3DOm carbon after four synthesis cycles (XRD pattern and HRTEM image of 3DOm-i LTL are shown in Figures S8 and S9, respectively). Unlike the other 3DOm-i zeolites discussed above, SAED of the LTL sample reveals a polycrystalline diffraction pattern which indicates very small crystal size of the LTL sample. As discussed in ref 12, the crystal size of zeolites grown by confinement can be varied by changing the relative magnitude of nucleation and crystal growth rates. Larger single crystals are formed when crystal growth is dominant, while zeolite nanocrystals composed of only one or a few spherical elements could be formed when abundant nucleation occurs in the initial synthesis cycle and crystal growth is relatively slow. The latter appears to be the case for LTL. The difference between the LTL sample and the other 3DOm-i zeolites clearly reveals how a wide range of crystal morphologies of zeolites can be achieved by tuning the nucleation and crystal growth rate in the confined space of the 3DOm carbon.

To further study the versatility of the synthesis approach, commercial carbon black (BP2000, Cabot Corp.) was selected as a disordered mesoporous carbon template for the confined synthesis of LTA and MFI (silicalite-1). SEM images in Figure S10 reveal the presence of disordered mesopores imprinted from the carbon black template. The mesopore structure is further confirmed by the nitrogen adsorption-desorption isotherms (not shown). Textural analysis (Table S1) indicates that their micropore volumes are similar to those of conventional zeolites. As expected, no diffraction peaks from the low-angle XRD patterns (not shown) are observed because of the disordered mesopore structure of the commercial carbon black.

In summary, BEA, LTA, FAU, and LTL zeolites with ordered mesoporosity have been synthesized within the confined space of 3DOm carbon by conventional hydrothermal treatment. The mesoporosity can be easily tuned by varying the mesopore size of 3DOm carbon and mesoporous structure of the carbon template, and a wide range of crystal morphologies can be achieved by varying the nucleation and crystal growth rate. The method is straightforward but time-consuming and costly. Therefore, we do not foresee its viability for commercial implementation for the preparation of catalysts or other materials with requirements of low cost per unit mass. However, this method may be appropriate for emerging applications of zeolites. For example, it has been demonstrated elsewhere that disassembly of 3DOm-i zeolites is a reliable method for obtaining suspensions of monodisperse zeolite nanocrystals with size range and uniformity that cannot be achieved by direct synthesis.[12] Therefore, the materials reported here could be useful for the formation of thin films and membranes[19] for which much higher costs per unit mass could be afforded. Moreover, it is believed that the ordered mesoporous zeolites could form a set of materials for fundamental studies of the effect of hierarchical mesopore structures on catalytic performance of zeolite catalysts. It is reasonable to expect that the synthesis approach demonstrated here will be applicable to other zeolites, facilitating the emergence of new hierarchical porous materials and their related applications in catalysis and separation.

■ ASSOCIATED CONTENT

Supporting Information. Experimental details; synthesis of 3DOm-i zeolites; and additional XRD, TEM, SEM, and porosity analyses. This material is available free of charge via the Internet at http://pubs.acs.org.

■ AUTHOR INFORMATION

Corresponding Author
wfan@ecs.umass.edu; tsapatsis@umn.edu

■ ACKNOWLEDGMENT

H.C. thanks the China Scholarship Council (CSC, 2009615071) for a fellowship to support his 2-year stay at UMN. This work was supported as part of the Catalysis Center for Energy Innovation, an Energy Frontier Research Center funded by the U.S. Department of Energy, Office of Science, Office of Basic Energy Sciences, under Award No. DE-SC0001004.

■ REFERENCES

(1) Davis, M. E. *Nature* **2002**, *417*, 813–821.
(2) (a) Cejka, J.; Mintova, S. *Catal. Rev. Sci. Eng.* **2007**, *49*, 457–509. (b) Perez-Ramirez, J.; Christensen, C. H.; Egeblad, K.; Christensen, C. H.; Groen, J. C. *Chem. Soc. Rev.* **2008**, *37*, 2530–2542. (c) Tao, Y. S.; Kanoh, H.; Abrams, L.; Kaneko, K. *Chem. Rev.* **2006**, *106*, 896–910.
(3) Hartmann, M. *Angew. Chem., Int. Ed.* **2004**, *43*, 5880–5882.
(4) Triantafyllidis, K. S.; Vlessidis, A. G.; Nalbandian, L.; Evmiridis, N. P. *Microporous Mesoporous Mater.* **2001**, *47*, 369–388.
(5) Groen, J. C.; Moulijn, J. A.; Perez-Ramirez, J. *J. Mater. Chem.* **2006**, *16*, 2121–2131.
(6) Ordomsky, V. V.; Murzin, V. Y.; Monakhova, Y. V.; Zubavichus, Y. V.; Knyazeva, E. E.; Nesterenko, N. S.; Ivanova, I. I. *Microporous Mesoporous Mater.* **2007**, *105*, 101–110.

(7) (a) Zhang, Z. T.; Han, Y.; Zhu, L.; Wang, R. W.; Yu, Y.; Qiu, S. L.; Zhao, D. Y.; Xiao, F. S. *Angew. Chem., Int. Ed.* **2001**, *40*, 1258–1261. (b) Liu, Y.; Zhang, W. Z.; Pinnavaia, T. J. *J. Am. Chem. Soc.* **2000**, *122*, 8791–8792.

(8) (a) Choi, M.; Cho, H. S.; Srivastava, R.; Venkatesan, C.; Choi, D. H.; Ryoo, R. *Nat. Mater.* **2006**, *5*, 718–723. (b) Choi, M.; Na, K.; Kim, J.; Sakamoto, Y.; Terasaki, O.; Ryoo, R. *Nature* **2009**, *461*, 246–249. (c) Na, K.; Choi, M.; Park, W.; Sakamoto, Y.; Terasaki, O.; Ryoo, R. *J. Am. Chem. Soc.* **2010**, *132*, 4169–4177. (d) Wang, J.; Groen, J. C.; Yue, W.; Zhou, W.; Coppens, M. O. *Chem. Commun.* **2007**, 4653–4655. (e) Lee, S. J.; Shantz, D. F. *Chem. Mater.* **2005**, *17*, 409–417. (f) Mukti, R. R.; Hirahara, H.; Sugawara, A.; Shimojima, A.; Okubo, T. *Langmuir* **2010**, *26*, 2731–2735.

(9) (a) Schmidt, I.; Madsen, C.; Jacobsen, C. J. H. *Inorg. Chem.* **2000**, *39*, 2279–2283. (b) Schmidt, I.; Boisen, A.; Gustavsson, E.; Stahl, K.; Pehrson, S.; Dahl, S.; Carlsson, A.; Jacobsen, C. J. H. *Chem. Mater.* **2001**, *13*, 4416–4418. (c) Yang, Z. X.; Xia, Y. D.; Mokaya, R. *Adv. Mater.* **2004**, *16*, 727–732.

(10) Fan, W.; Snyder, M. A.; Kumar, S.; Lee, P. S.; Yoo, W. C.; McCormick, A. V.; Penn, R. L.; Stein, A.; Tsapatsis, M. *Nat. Mater.* **2008**, *7*, 984–991.

(11) Liu, D.; Bhan, A.; Tsapatsis, M.; Al Hashimi, S. *ACS Catal.* **2010**, *1*, 7–17.

(12) Lee, P. S.; Zhang, X.; Stoeger, J. A.; Malek, A.; Fan, W.; Kumar, S.; Yoo, W. C.; Al Hashimi, S.; Penn, R. L.; Stein, A.; Tsapatsis, M. *J. Am. Chem. Soc.* **2010**, *133*, 493–502.

(13) Xu, W. Y.; Dong, J. X.; Li, J. P.; Li, J. Q.; Wu, F. *J. Chem. Soc., Chem. Commun.* **1990**, 755–756.

(14) (a) Matsukata, M.; Ogura, M.; Osaki, T.; Rao, P.; Nomura, M.; Kikuchi, E. *Top. Catal.* **1999**, *9*, 77–92. (b) Matsukata, M.; Osaki, T.; Ogura, M.; Kikuchi, E. *Microporous Mesoporous Mater.* **2002**, *56*, 1–10.

(15) (a) Davis, T. M.; Snyder, M. A.; Krohn, J. E.; Tsapatsis, M. *Chem. Mater.* **2006**, *18*, 5814–5816. (b) Snyder, M. A.; Lee, J. A.; Davis, T. M.; Scriven, L. E.; Tsapatsis, M. *Langmuir* **2007**, *23*, 9924–9928. (c) Yokoi, T.; Sakamoto, Y.; Terasaki, O.; Kubota, Y.; Okubo, T.; Tatsumi, T. *J. Am. Chem. Soc.* **2006**, *128*, 13664–13665.

(16) Mintova, S.; Valtchev, V.; Onfroy, T.; Marichal, C.; Knözinger, H.; Bein, T. *Microporous Mesoporous Mater.* **2006**, *90*, 237–245.

(17) Jon, H.; Lu, B. W.; Oumi, Y.; Itabashi, K.; Sano, T. *Microporous Mesoporous Mater.* **2006**, *89*, 88–95.

(18) (a) Fan, W.; Ogura, M.; Sankar, G.; Okubo, T. *Chem. Mater.* **2007**, *19*, 1906–1917. (b) Fan, W.; Shirato, S.; Gao, F.; Ogura, M.; Okubo, T. *Microporous Mesoporous Mater.* **2006**, *89*, 227–234. (c) Tsapatsis, M.; Lovallo, M.; Okubo, T.; Davis, M. E.; Sadakata, M. *Chem. Mater.* **1995**, *7*, 1734–1741.

(19) (a) Lew, C. M.; Cai, R.; Yan, Y. S. *Acc. Chem. Res.* **2010**, *43*, 210–219. (b) Lai, Z. P.; Bonilla, G.; Diaz, I.; Nery, J. G.; Sujaoti, K.; Amat, M. A.; Kokkoli, E.; Terasaki, O.; Thompson, R. W.; Tsapatsis, M.; Vlachos, D. G. *Science* **2003**, *300*, 456–460.